

Optimizing the basis of $B \rightarrow K^* l^+ l^-$ observables and understanding its tensions

Joaquim Matias
Universitat Autònoma de Barcelona

EPS 2013, Stockholm

Based on: S. Descotes-Genon, T. Hurth, JM, J. Virto, [JHEP 1305 \(2013\) 137](#)
S. Descotes-Genon, JM, J. Virto, [in preparation](#)

July 19, 2013

PLAN of the TALK

- Why is so important the measurement of $B \rightarrow K^*(\rightarrow K\pi)l^+l^-$?
- The path towards an optimized basis of observables to describe this 4-body decay.
- First analysis of new data on $P_{1,2}$ and understanding of its tensions (3σ).
- Conclusions

⇒ In the short term the best paradigm to unveil **New Physics** will be an accurate analysis of Wilson coefficients.

- UT for CPV \leftrightarrow *Wilson Coefficient* correlations for Rare Decays
- Wilson Coefficients are tested $C_i = C_i^{SM} + \delta C_i$ $\left\{ \begin{array}{l} \text{different levels of accuracy} \\ \text{allow different ranges of NP} \end{array} \right.$

<u>Wilson coefficients</u>	<u>Observables</u>	<u>SM values</u>
$C_7^{\text{eff}}(\mu_b)$	$\mathcal{B}(\bar{B} \rightarrow X_s \gamma), A_I(B \rightarrow K^* \gamma), S_{K^* \gamma}, A_{FB}, F_L$	-0.292
$C_9(\mu_b)$	$\mathcal{B}(B \rightarrow X_s \ell \ell), A_{FB}, F_L$	4.075
$C_{10}(\mu_b)$	$\mathcal{B}(B_s \rightarrow \mu^+ \mu^-), \mathcal{B}(B \rightarrow X_s \ell \ell), A_{FB}, F_L$	-4.308
$C_7'(\mu_b)$	$\mathcal{B}(\bar{B} \rightarrow X_s \gamma), A_I(B \rightarrow K^* \gamma), S_{K^* \gamma}, A_{FB}, F_L$	-0.006
$C_9'(\mu_b)$	$\mathcal{B}(B \rightarrow X_s \ell \ell), A_{FB}, F_L$	0
$C_{10}'(\mu_b)$	$\mathcal{B}(B_s \rightarrow \mu^+ \mu^-), A_{FB}, F_L$	0

High Precision Observables are necessary to disentangle NP and to **overconstrain** the deviations δC_i of Wilson Coefficients from SM in order to reduce allowed regions.

⇒ In the short term the best paradigm to unveil **New Physics** will be an accurate analysis of Wilson coefficients.

- UT for CPV \leftrightarrow *Wilson Coefficient* correlations for Rare Decays
- Wilson Coefficients are tested $C_i = C_i^{SM} + \delta C_i$ $\left\{ \begin{array}{l} \text{different levels of accuracy} \\ \text{allow different ranges of NP} \end{array} \right.$

<u>Wilson coefficients</u>	<u>Observables</u>	<u>SM values</u>
$C_7^{\text{eff}}(\mu_b)$	$\mathcal{B}(\bar{B} \rightarrow X_s \gamma), A_I(B \rightarrow K^* \gamma), S_{K^* \gamma}, A_{FB}, F_L, P_2, P'_{4,5}$	-0.292
$C_9(\mu_b)$	$\mathcal{B}(B \rightarrow X_s \ell \ell), A_{FB}, F_L, P_2, P'_{4,5}$	4.075
$C_{10}(\mu_b)$	$\mathcal{B}(B_s \rightarrow \mu^+ \mu^-), \mathcal{B}(B \rightarrow X_s \ell \ell), A_{FB}, F_L, P'_4$	-4.308
$C'_7(\mu_b)$	$\mathcal{B}(\bar{B} \rightarrow X_s \gamma), A_I(B \rightarrow K^* \gamma), S_{K^* \gamma}, A_{FB}, F_L, P_1$	-0.006
$C'_9(\mu_b)$	$\mathcal{B}(B \rightarrow X_s \ell \ell), A_{FB}, F_L, P_1$	0
$C'_{10}(\mu_b)$	$\mathcal{B}(B_s \rightarrow \mu^+ \mu^-), A_{FB}, F_L, P_1, P'_4$	0

High Precision Observables are necessary to disentangle NP and to **overconstrain** the deviations δC_i of Wilson Coefficients from SM in order to reduce allowed regions.

⇒ $B \rightarrow K^*(\rightarrow K\pi)\mu^+\mu^-$ fulfills the requirements by means of **clean observables** $P_{1,2,3}, P'_{4,5,6,8}$ improving the precision in not very accurately constrained coefficients like C_9 or $C'_{7,9,10}$ (soon).
 New Physics in phases of Wilson Coefficients: $P_3, P'_{6,8}$.

All those observables come from the decay $\bar{B}_d \rightarrow \bar{K}^{*0}(\rightarrow K^-\pi^+)l^+l^-$ with the K^{*0} on the mass shell. It is described by $s = q^2$ and three angles θ_l , θ_K and ϕ

$$\frac{d^4\Gamma(\bar{B}_d)}{dq^2 d\cos\theta_l d\cos\theta_K d\phi} = \frac{9}{32\pi} J(q^2, \theta_l, \theta_K, \phi)$$

The differential distribution splits in J_i coefficients:

$$\begin{aligned} J(q^2, \theta_l, \theta_K, \phi) = & J_{1s} \sin^2 \theta_K + J_{1c} \cos^2 \theta_K + (J_{2s} \sin^2 \theta_K + J_{2c} \cos^2 \theta_K) \cos 2\theta_l + J_3 \sin^2 \theta_K \sin^2 \theta_l \cos 2\phi \\ & + J_4 \sin 2\theta_K \sin 2\theta_l \cos \phi + J_5 \sin 2\theta_K \sin \theta_l \cos \phi + (J_{6s} \sin^2 \theta_K + J_{6c} \cos^2 \theta_K) \cos \theta_l \\ & + J_7 \sin 2\theta_K \sin \theta_l \sin \phi + J_8 \sin 2\theta_K \sin 2\theta_l \sin \phi + J_9 \sin^2 \theta_K \sin^2 \theta_l \sin 2\phi. \end{aligned}$$

There is a corresponding CP - conjugate distribution for $B_d \rightarrow K^{*0}(\rightarrow K^-\pi^+)l^+l^-$ function of \bar{J} .

The information on

- the transversity amplitudes of the K^* ($A_{\perp,\parallel,0}$) is inside the coefficients J_i .
- short distance physics C_i is encoded in ($A_{\perp,\parallel,0} = C_i \times \text{form factors}$)

$$\begin{aligned}
J_{1s} &= \frac{(2 + \beta_\ell^2)}{4} \left[|A_\perp^L|^2 + |A_\parallel^L|^2 + (L \rightarrow R) \right] + \frac{4m_\ell^2}{q^2} \text{Re} \left(A_\perp^L A_\perp^{R*} + A_\parallel^L A_\parallel^{R*} \right), \\
J_{1c} &= |A_0^L|^2 + |A_0^R|^2 + \frac{4m_\ell^2}{q^2} \left[|A_t|^2 + 2\text{Re}(A_0^L A_0^{R*}) \right] + \beta_\ell^2 |A_S|^2, \\
J_{2s} &= \frac{\beta_\ell^2}{4} \left[|A_\perp^L|^2 + |A_\parallel^L|^2 + (L \rightarrow R) \right], \quad J_{2c} = -\beta_\ell^2 \left[|A_0^L|^2 + (L \rightarrow R) \right], \\
J_3 &= \frac{1}{2} \beta_\ell^2 \left[|A_\perp^L|^2 - |A_\parallel^L|^2 + (L \rightarrow R) \right], \quad J_4 = \frac{1}{\sqrt{2}} \beta_\ell^2 \left[\text{Re}(A_0^L A_\parallel^{L*}) + (L \rightarrow R) \right], \\
J_5 &= \sqrt{2} \beta_\ell \left[\text{Re}(A_0^L A_\perp^{L*}) - (L \rightarrow R) - \frac{m_\ell}{\sqrt{q^2}} \text{Re}(A_\parallel^L A_S^* + A_\parallel^R A_S^*) \right], \\
J_{6s} &= 2\beta_\ell \left[\text{Re}(A_\parallel^L A_\perp^{L*}) - (L \rightarrow R) \right], \quad J_{6c} = 4\beta_\ell \frac{m_\ell}{\sqrt{q^2}} \text{Re} \left[A_0^L A_S^* + (L \rightarrow R) \right], \\
J_7 &= \sqrt{2} \beta_\ell \left[\text{Im}(A_0^L A_\parallel^{L*}) - (L \rightarrow R) + \frac{m_\ell}{\sqrt{q^2}} \text{Im}(A_\perp^L A_S^* + A_\perp^R A_S^*) \right], \\
J_8 &= \frac{1}{\sqrt{2}} \beta_\ell^2 \left[\text{Im}(A_0^L A_\perp^{L*}) + (L \rightarrow R) \right], \quad J_9 = \beta_\ell^2 \left[\text{Im}(A_\parallel^{L*} A_\perp^L) + (L \rightarrow R) \right]
\end{aligned}$$

In **red** lepton mass terms ($\beta_\ell^2 = 1 - 4m_\ell^2/q^2$).

[Egede, Hurth, JM, Ramon, Reece'10]

An important step forward to find a complete description of the distribution was the identification of the **symmetries** of the distribution:

Transformation of amplitudes leaving distribution invariant.

Symmetries determine the minimal # observables for each scenario:

$$n_{obs} = 2n_A - n_S$$

Case	Coefficients	Amplitudes	Symmetries	Observables
$m_\ell = 0, A_S = 0$	11	6	4	8 \Leftarrow
$m_\ell = 0$	11	7	5	9
$m_\ell > 0, A_S = 0$	11	7	4	10
$m_\ell > 0$	12	8	4	12

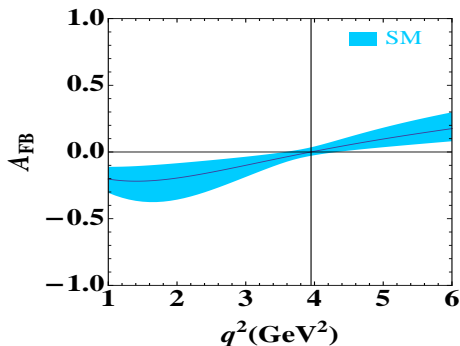
All symmetries (massive and scalars) were found explicitly later on. [JM, Mescia, Ramon, Virto'12]

Symmetries \Rightarrow # of observables \Rightarrow determine a **basis**: each angular observable constructed can be expressed in terms of this basis.

Main criteria to define this basis: **minimize the form factor sensitivity**

The concept of clean observables

For a long time huge efforts were devoted (still now) to measure the position of the zero of the forward-backward asymmetry A_{FB} of $B \rightarrow K^* \mu^+ \mu^-$.



Reason:

- At LO the soft form factor dependence ($\xi_{\perp}(q^2), \xi_{\parallel}(q^2)$) cancels exactly at the position of the zero q_0^2 (dependence appears at NLO).
- A relation among $\mathbf{C}_9^{\text{eff}}$ and $\mathbf{C}_7^{\text{eff}}$ arises at the zero (at LO):

$$\mathbf{C}_9^{\text{eff}}(q_0^2) + 2 \frac{m_b M_B}{q_0^2} \mathbf{C}_7^{\text{eff}} = 0$$

A similar idea was incorporated in the construction of the transverse asymmetry

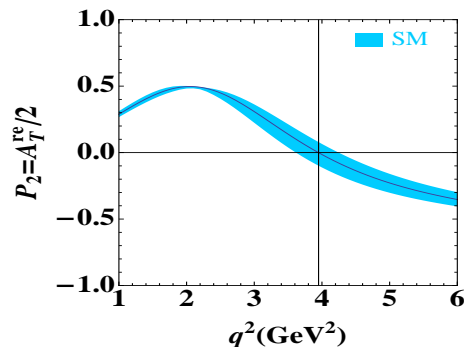
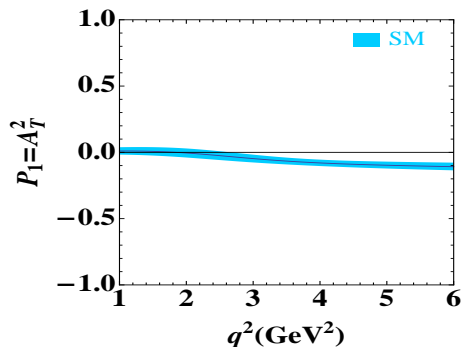
[Kruger, J.M'05]

$$P_1 = A_T^{(2)}(q^2) = \frac{|A_\perp|^2 - |A_\parallel|^2}{|A_\perp|^2 + |A_\parallel|^2}$$

[Becirevic et al.'12]

$$P_2 = \frac{A_T^{re}}{2} = \frac{\text{Re}(A_\perp^{L*} A_\parallel^L - A_\perp^R A_\parallel^{R*})}{|A_\perp|^2 + |A_\parallel|^2}$$

where $A_{\perp,\parallel}$ correspond to two transversity amplitudes of the K^* .



- Both asymmetries exhibit an exact cancellation of soft form factors **not only at a point** (like A_{FB}) **but in the full low- q^2 range** (0.1 – 6 GeV²).
- First examples of **clean** observables that could be measured.
- $A_T^{(2)}$ is constructed to detect presence of RH currents ($A_\perp \sim -A_\parallel$ in the SM), A_T^{re} complements (partly supersedes) A_{FB} since it contains similar information, but in a theoretically better controlled way.

[Egede, Hurth, JM, Ramon, Reece'08, and '10]

- Later on a set of **transverse asymmetries** called $\mathbf{A}_T^{(3,4,5)}$ were proposed

$$\mathbf{A}_T^{(3)} = \frac{|A_0^L A_{\parallel}^{L*} + A_0^{R*} A_{\parallel}^R|}{\sqrt{|A_0|^2 |A_{\perp}|^2}} \quad \mathbf{A}_T^{(4)} = \frac{|A_0^L A_{\perp}^{L*} - A_0^{R*} A_{\perp}^R|}{|A_0^L A_{\parallel}^{L*} + A_0^{R*} A_{\parallel}^R|} \quad \mathbf{A}_T^{(5)} = \frac{|A_{\perp}^L A_{\parallel}^{R*} + A_{\perp}^{R*} A_{\parallel}^L|}{|A_{\perp}|^2 + |A_{\parallel}|^2}$$

[Bobeth, Hiller, Dyk, '10]

- Also at the low-recoil a set of clean observables called $\mathbf{H}_T^{(1,2,3)}$ were proposed that correspond to $P_{4,5,6}$ at large-recoil.

$$\mathbf{H}_T^{(1)} = \frac{\text{Re}(A_0^L A_{\parallel}^{L*} + A_0^{R*} A_{\parallel}^R)}{\sqrt{|A_0|^2 |A_{\parallel}|^2}}, \quad \mathbf{H}_T^{(2)} = \frac{\text{Re}(A_0^L A_{\perp}^{L*} - A_0^{R*} A_{\perp}^R)}{\sqrt{|A_0|^2 |A_{\perp}|^2}}, \quad \mathbf{H}_T^{(3)} = \frac{\text{Re}(A_{\parallel}^L A_{\perp}^{L*} - A_{\parallel}^{R*} A_{\perp}^R)}{\sqrt{|A_{\parallel}|^2 |A_{\perp}|^2}}$$

[Altmannshofer, Ball, Bharucha, Buras, Straub, Wick'09]

- In parallel a set of CP-conserving and CP-violating observables \mathbf{S}_i and \mathbf{A}_i were constructed directly from the coefficients of the distribution, easy to measure but **not** following the criteria of **clean observables**:

$$\mathbf{S}_i = \frac{\int_{bin} dq^2 [J_i + \bar{J}_i]}{d\Gamma/dq^2 + d\bar{\Gamma}/dq^2}, \quad \mathbf{A}_i = \frac{\int_{bin} dq^2 [J_i - \bar{J}_i]}{d\Gamma/dq^2 + d\bar{\Gamma}/dq^2}.$$

Finally we arrived to an **Optimal Basis** of observables, a compromise between:

- *Excellent experimental accessibility and simplicity of the fit.*
- *Reduced FF dependence (in the large-recoil region: $0.1 \leq q^2 \leq 8 \text{ GeV}^2$).*

Our proposal for **CP-conserving basis**:

$$\left\{ \frac{d\Gamma}{dq^2}, \mathbf{A}_{\text{FB}}, \mathbf{P}_1, \mathbf{P}_2, \mathbf{P}_3, \mathbf{P}'_4, \mathbf{P}'_5, \mathbf{P}'_6 \right\} \text{ or } \mathbf{P}_3 \leftrightarrow \mathbf{P}'_8 \text{ and } \mathbf{A}_{\text{FB}} \leftrightarrow \mathbf{F}_L$$

where $P_1 = A_T^2$ [Kruger, J.M'05], $P_2 = \frac{1}{2}A_T^{\text{re}}$, $P_3 = -\frac{1}{2}A_T^{\text{im}}$ [Becirevic, Schneider'12] and $P'_{4,5,6}$ [Descotes, JM, Ramon, Virto'13]) given by

$$P'_i = \frac{1}{k_i N_i} [J_i + \bar{J}_i] \quad N_i = \sqrt{-(J_{2s} + \bar{J}_{2s})(J_{2c} + \bar{J}_{2c})} \quad k_4 = 1, k_5 = 2, k_6 = -2$$

and the corresponding **CP-violating basis** ($J_i + \bar{J}_i \rightarrow J_i - \bar{J}_i$ in numerators):

$$\{ \mathbf{A}_{\text{CP}}, \mathbf{A}_{\text{FB}}^{\text{CP}}, \mathbf{P}_1^{\text{CP}}, \mathbf{P}_2^{\text{CP}}, \mathbf{P}_3^{\text{CP}}, \mathbf{P}_4^{\text{CP}}, \mathbf{P}_5^{\text{CP}}, \mathbf{P}_6^{\text{CP}} \} \text{ or } \mathbf{P}_3^{\text{CP}} \leftrightarrow \mathbf{P}_8^{\text{CP}} \text{ and } \mathbf{A}_{\text{FB}}^{\text{CP}} \leftrightarrow \mathbf{F}_L^{\text{CP}}$$

Large-recoil: NLO QCD factorization + $\mathcal{O}(\Lambda/m_b)$. Soft form factors $\xi_{\perp,\parallel}(q^2)$ from

$$\xi_{\perp}(q^2) = m_B/(m_B + m_{K^*}) \mathbf{V}(\mathbf{q}^2) \quad \xi_{\parallel}(q^2) = (m_B + m_{K^*})/(2E) \mathbf{A}_1(\mathbf{q}^2) - (m_B - m_{K^*})/(m_B) \mathbf{A}_2(\mathbf{q}^2)$$

- FF at $q^2 = 0$ and slope parameters are computed by [Khodjamirian et al.'10] (**KMPW**) using LCSR.

Tensor form factors $\mathbf{T}_{\perp,\parallel}$ are computed in QCDF following [Beneke, Feldmann, Seidel'01,'05] including factorizable and non-factorizable contributions.

Low-recoil: LCSR are valid up to $q^2 \leq 14 \text{ GeV}^2$. We extend FF determination [Bobeth & Hiller & Dyk'10] till 19 GeV^2 and cross check the consistency with **lattice** QCD.

In HQET one expects the ratios to be near one

$$\mathbf{R}_1 = \frac{\mathbf{T}_1(\mathbf{q}^2)}{\mathbf{V}(\mathbf{q}^2)}, \quad \mathbf{R}_2 = \frac{\mathbf{T}_2(\mathbf{q}^2)}{\mathbf{A}_1(\mathbf{q}^2)}, \quad \mathbf{R}_3 = \frac{q^2}{m_B^2} \frac{T_3(q^2)}{A_2(q^2)}.$$

Our approach at low-recoil: we determine $T_{1,2}$ by exploiting the ratios $R_{1,2}$ allowing for up to a 20% breaking, i.e., $R_{1,2} = 1 + \delta_{1,2}$. All other form factors extrapolated from KMPW. We find perfect agreement between our determination of $T_{1,2}$ using $R_{1,2}$ and lattice data.

Contact between theory and experiment:

Indeed the observables are measured in bins.

Present bins: [0.1,2], [2,4.3], [4.3,8.68], [1,6], [14.18,16], [16,19] GeV².

This requires a **redefinition** of observables in **bins**: $\langle J_i \rangle_{\text{bin}} = \int_{\text{bin}} [J_i + \bar{J}_i] dq^2$

$$\langle A_T^{(2)} \rangle_{\text{bin}} \equiv \langle P_1 \rangle_{\text{bin}} = \frac{\langle J_3 \rangle_{\text{bin}}}{2 \langle J_{2s} \rangle_{\text{bin}}} \quad \langle P_2 \rangle_{\text{bin}} = \frac{\langle J_{6s} \rangle_{\text{bin}}}{8 \langle J_{2s} \rangle_{\text{bin}}} \quad \langle P_3 \rangle_{\text{bin}} = -\frac{\langle J_9 \rangle_{\text{bin}}}{4 \langle J_{2s} \rangle_{\text{bin}}}$$

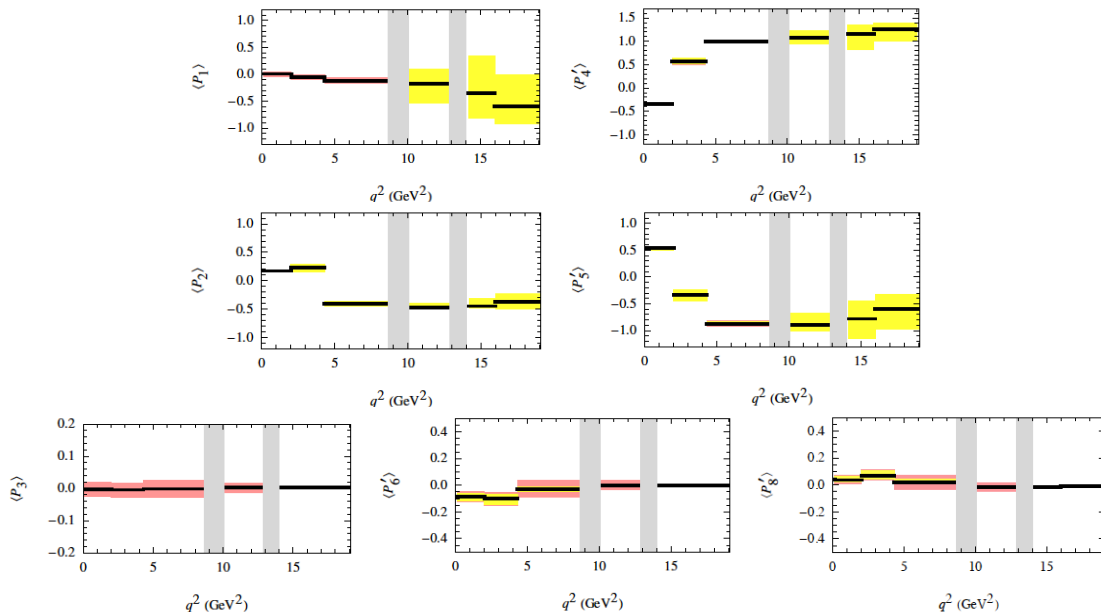
$$\langle P'_4 \rangle_{\text{bin}} = \frac{\langle J_4 \rangle_{\text{bin}}}{\sqrt{-\langle J_{2s} \rangle_{\text{bin}} \langle J_{2c} \rangle_{\text{bin}}}} \quad \langle P'_5 \rangle_{\text{bin}} = \frac{\langle J_5 \rangle_{\text{bin}}}{2\sqrt{-\langle J_{2s} \rangle_{\text{bin}} \langle J_{2c} \rangle_{\text{bin}}}} \quad \langle P'_6 \rangle_{\text{bin}} = \frac{-\langle J_7 \rangle_{\text{bin}}}{2\sqrt{-\langle J_{2s} \rangle_{\text{bin}} \langle J_{2c} \rangle_{\text{bin}}}}.$$

Similar definitions for $\langle P_i^{CP} \rangle_{\text{bin}}$ with $J_i - \bar{J}_i$.

$P_{1,2,3}$ were first indirectly measured via S_3, A_{im}, A_{FB}, F_L
(and already provide constraints).

First results on $P_{1,2}$ available since Beauty 2013.

BUT it is urgent to get experimental measurements of P'_i

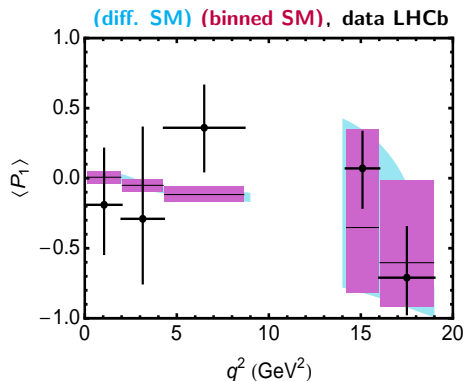


First measurement and analysis of P_1, P_2

R. Aaij et al. LHCb, 1304.6325 [hep-ex]

At Beauty $P_{1,2}$ were presented. Conclusion: Results consistent with SM predictions. BUT ...

Regarding measurement of P_1 at LHCb:



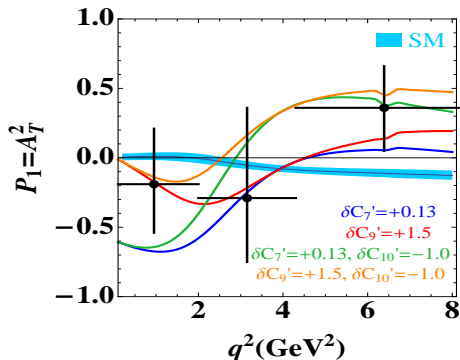
- Three first bins same 'shape' as CDF.
- Why error bars so large?
- **Too early to draw any definite conclusion on existence or not of right-handed currents.**

We suggest a new folding to measure uniquely P_1 .

$$d\Gamma(\hat{\phi}, \hat{\theta}_\ell, \hat{\theta}_K) + d\Gamma(\hat{\phi}, \hat{\theta}_\ell, \pi - \hat{\theta}_K) + d\Gamma(-\hat{\phi}, \pi - \hat{\theta}_\ell, \hat{\theta}_K) + d\Gamma(-\hat{\phi}, \pi - \hat{\theta}_\ell, \pi - \hat{\theta}_K) = f(P_1, F_L) + g(A_S^5, A_S^8)$$

At Beauty $P_{1,2}$ were presented. Conclusion: Results consistent with SM predictions. BUT ...

Regarding measurement of P_1 at LHCb:



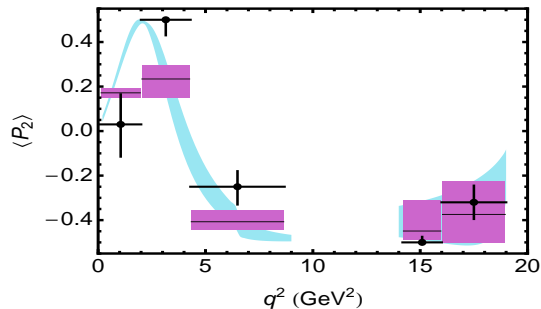
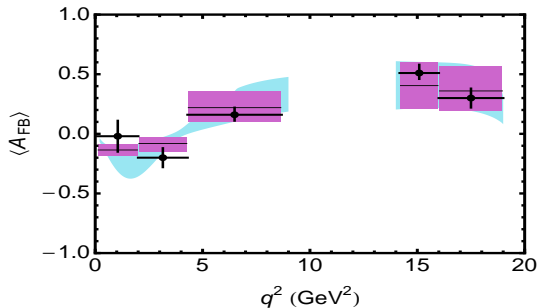
- Three first bins same 'shape' as CDF.
- Why error bars so large?
- **Too early to draw any definite conclusion on existence or not of right-handed currents.**
- P_1 can discriminate clearly **at large recoil** on the presence of $\delta C_7'$, $\delta C_9'$ and $\delta C_{10}'$ if error bars reduced:
 - $\delta C_7' > 0$ (a bit large) **BLUE**
 - $\delta C_9' > 0$ also can generate it. **RED**
 - $\delta C_{10}' < 0$ together with ($\delta C_7' > 0$ **GREEN** or $\delta C_9' > 0$ **ORANGE**) can reproduce the shape easily.

We suggest a new folding to measure uniquely P_1 .

$$d\Gamma(\hat{\phi}, \hat{\theta}_\ell, \hat{\theta}_K) + d\Gamma(\hat{\phi}, \hat{\theta}_\ell, \pi - \hat{\theta}_K) + d\Gamma(-\hat{\phi}, \pi - \hat{\theta}_\ell, \hat{\theta}_K) + d\Gamma(-\hat{\phi}, \pi - \hat{\theta}_\ell, \pi - \hat{\theta}_K) = f(P_1, F_L) + g(A_S^5, A_S^8)$$

First measurement and analysis of P_1, P_2

Concerning the forward-back asymmetry (A_{FB}) and P_2 :



- P_2 is the evolved version of A_{FB} , but, they play a complementary role.
- It magnifies a tiny tension in the second bin of A_{FB} .
- Both zeroes prefer a higher value $q_0^{2exp} = 4.9 \pm 0.9$ GeV² compared to $q_0^{2SM} = 3.95 \pm 0.38$ GeV².

At LO how to move the position of the zero to the right?

$$q_0^{2LO} = -2m_b M_B \frac{C_7^{eff} C_{10} - C_7' C_{10}'}{C_9^{eff} (q_0^2) C_{10} - C_9' C_{10}'}$$

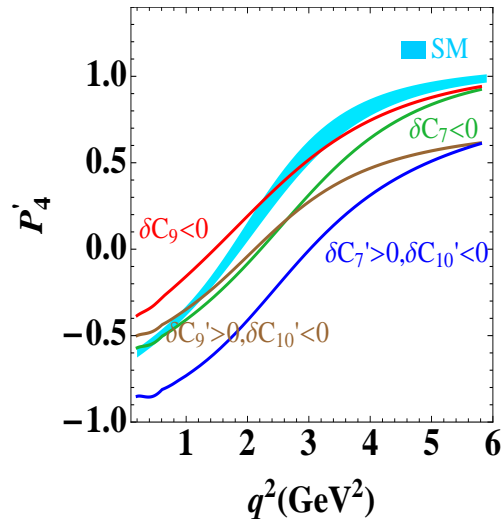
where $C_i = C_i^{SM} + \delta C_i$

Four main possibilities on how to test them:

Mechanism	Constraint: A_{FB} in 3 bins	Constraint: P_2 in 3 bins	Constraint: P_1 in 3 bins
I. $\delta C_7 < 0$	OK	OK	\sim
II. $\delta C_9 < 0$	OK	OK	\sim
III. $(\delta C_7' > 0, \delta C_{10}' < 0)$	OK	\sim	OK
IV. $(\delta C_7' < 0, \delta C_{10}' > 0)$	NO	\sim	NO
V. $(\delta C_9' > 0, \delta C_{10}' < 0)$	OK	\sim	OK
VI. $(\delta C_9' < 0, \delta C_{10}' > 0)$	NO	\sim	NO

Mechanism I, II, III and V preferred.

- $\delta C_7 < 0$ preferred by radiative constraints.
- $\delta C_9 < 0$, mechanism mainly tested with P_5'
- Mec. III-VI sign of $\delta C_{10}'$ tested by P_4' and P_1 .
- Mec. III-IV sign of $\delta C_7'$ tested by P_1
- Mec. V, $\delta C_9'$ can be tested by P_1 .



At LO how to move the position of the zero to the right?

$$q_0^{2LO} = -2m_b M_B \frac{C_7^{eff} C_{10} - C_7' C_{10}'}{C_9^{eff}(q_0^2) C_{10} - C_9' C_{10}'}$$

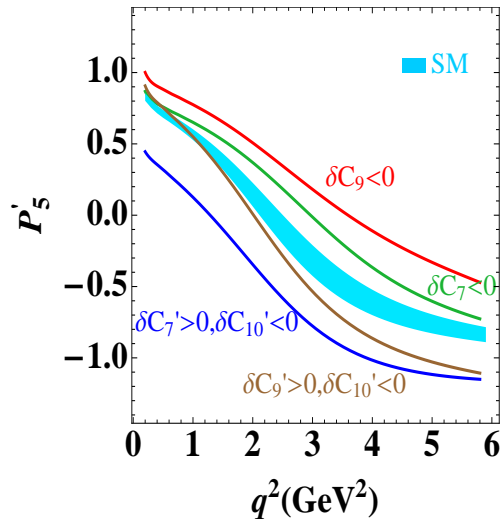
where $C_i = C_i^{SM} + \delta C_i$

Six main possibilities and how to test them:

Mechanism	Constraint: A_{FB} in 3 bins	Constraint: P_2 in 3 bins	Constraint: P_1 in 3 bins
I. $\delta C_7 < 0$	OK	OK	\sim
II. $\delta C_9 < 0$	OK	OK	\sim
III. $(\delta C_7' > 0, \delta C_{10}' < 0)$	OK	\sim	OK
IV. $(\delta C_7' < 0, \delta C_{10}' > 0)$	NO	\sim	NO
V. $(\delta C_9' > 0, \delta C_{10}' < 0)$	OK	\sim	OK
VI. $(\delta C_9' < 0, \delta C_{10}' > 0)$	NO	\sim	NO

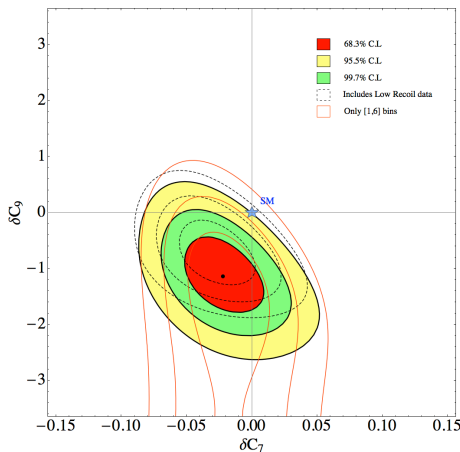
Mechanism I, II, III and V preferred.

- $\delta C_7 < 0$ preferred by radiative constraints.
- $\delta C_9 < 0$, mechanism mainly tested with P_5'
- Mec. III-VI sign of $\delta C_{10}'$ tested by P_4' and P_1 .
- Mec. III-IV sign of $\delta C_7'$ tested by P_1
- Mec. V, $\delta C_9'$ can be tested by P_1 .



After analyzing different scenarios we have performed a frequentist analysis with asymmetric errors and NP error bars to a scenario with δC_7 and δC_9 including: 1. $\mathcal{B}(B \rightarrow X_s \gamma)$, $A_I(B \rightarrow K^* \gamma)$, $S_{K^* \gamma}$, $\mathcal{B}(B \rightarrow X_s \mu^+ \mu^-)$ and $\mathcal{B}(B_s \rightarrow \mu^+ \mu^-)$ together with P_1 , P_2 , A_{FB} of $B \rightarrow K^* \mu^+ \mu^-$.

Result in $\delta C_7 - \delta C_9$:



We find 3σ deviation from SM prediction for C_9 (check the rest of basis P_i' !)

- 3 large-recoil bins (colored)
 $C_7 \in (-0.332, -0.287)$ and $C_9 \in (2.58, 3.38)$
- ONLY 1-6 bin at large recoil (orange)
- 3 large-recoil and 2 low-recoil bins (dashed)

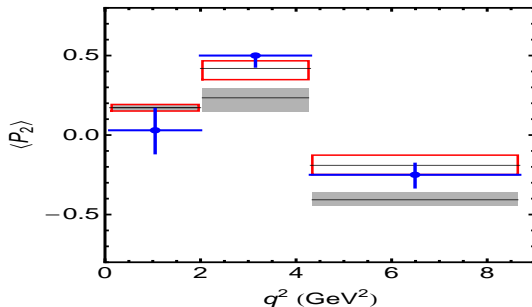
Robustness tests:

- We have checked using naive factorization that the effect on C_9 is confirmed.
- Also the bin 1-6 confirms the deviation.
- We have analyzed two types of charm effects:
 - m_c value: Increasing m_c up to 1.4 GeV reduces significance to 2.3σ .
 - non-perturbative $c - \bar{c}$ contribution (KMPW) increases slightly the significance above 3σ .

P_2 for **New Physics** $\delta C_9 = -1.5$ (**red box**)

SM binned prediction in **gray** \Rightarrow

LHCb data crosses in **blue**



For completeness we show also the result of full fit to all:

- $\delta C_{10}, \delta C'_{7,9,10}$ are already consistent with SM at 1σ
- δC_7 at 2σ
- δC_9 at 3σ

Coefficient	1σ	2σ	3σ
δC_7	$[-0.04, -0.01]$	$[-0.06, 0.01]$	$[-0.08, 0.03]$
δC_9	$[-1.2, -0.5]$	$[-1.5, -0.1]$	$[-1.8, 0.4]$
δC_{10}	$[0, +1.8]$	$[-0.8, 2.4]$	$[-1.8, 3.4]$
$\delta C'_7$	$[-0.05, 0.03]$	$[-0.1, 0.08]$	$[-0.14, 0.13]$
$\delta C'_9$	$[-0.2, 1]$	$[-0.8, 1.4]$	$[-1.4, 1.8]$
$\delta C'_{10}$	$[-0.8, 0.2]$	$[-1.4, 0.6]$	$[-2.0, 1.0]$

Table : 68.3% (1σ), 95.5% (2σ) and 99.7% (3σ) confidence intervals for the NP contributions to Wilson coefficients resulting from the global analysis.

Conclusions

- We have combined recent LHCb measurements on the first two theoretically clean observables $P_{1,2}$ of the optimal basis together with A_{FB} , other radiative modes and $B_s \rightarrow \mu^+ \mu^-$. We work in the framework of NLO QCD at large-recoil and HQET at low-recoil.
- **We have found a strong indication for a negative possible New Physics contribution to the coefficient C_9 at 3σ using large-recoil data and 2.6σ using both large and low-recoil data.** This result corresponds to a range for C_9 inside a 68% CL of $2.6 \leq C_9 \leq 3.4$ to be compared with the SM value for $C_9^{SM} = 4.075$ at same μ_b scale. Different robustness tests have been included.
- A too large error bars on P_1 does not allow **yet** to draw any definite conclusion on the existence or not of right-handed currents. Still in our global fit we do not see clear indications of the need to introduce them.

Prospects: A measurement of the rest of the basis P'_i is essential to disprove or confirm this result

BACK-UP SLIDES

Computation of Primary Observables

Large-recoil: NLO QCD factorization + $\mathcal{O}(\Lambda/m_b)$. Soft form factors $\xi_{\perp,\parallel}(q^2)$ from

$$\xi_{\perp}(q^2) = m_B/(m_B + m_{K^*}) \mathbf{V}(\mathbf{q}^2) \quad \xi_{\parallel}(q^2) = (m_B + m_{K^*})/(2E) \mathbf{A}_1(\mathbf{q}^2) - (m_B - m_{K^*})/(m_B) \mathbf{A}_2(\mathbf{q}^2)$$

- FF at $q^2 = 0$ and slope parameters are computed by [Khodjamirian et al.'10] (**KMPW**) using LCSR.

Tensor form factors $\mathcal{T}_{\perp,\parallel}$ are computed in QCDF following [Beneke, Feldmann, Seidel'01,'05] including factorizable and non-factorizable contributions.

The wide spread of different errors in literature associated to FF:

$$V(0) = 0.31 \pm 0.04 \text{ and } A(0) = 0.33 \pm 0.03 \text{ [W. Altmannshofer et al.'09]}$$

$$V(0) = 0.36 \pm 0.17 \text{ and } A(0) = 0.29 \pm 0.10 \text{ [A. Khodjamirian et al. '10].}$$

Even central values have shifted significantly $V(0) = 0.41 \pm 0.05$ [P. Ball and R. Zwicky,'05] (**BZ**).

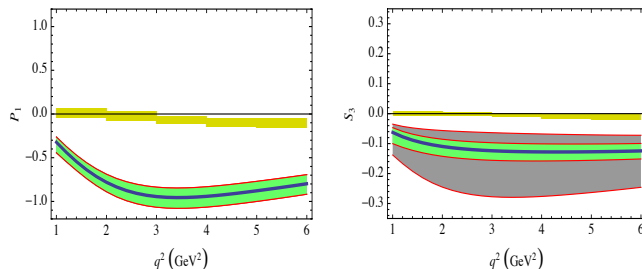


Figure : Predictions in SM and for one benchmark point of NP for P_1 (left) and S_3 (right). The yellow boxes are the SM predictions integrated in five 1 GeV² bins. The blue curve corresponds to the central values for the NP scenario. The green/grey band is the total uncertainty considering two different FF determinations (BZ/KMPW).

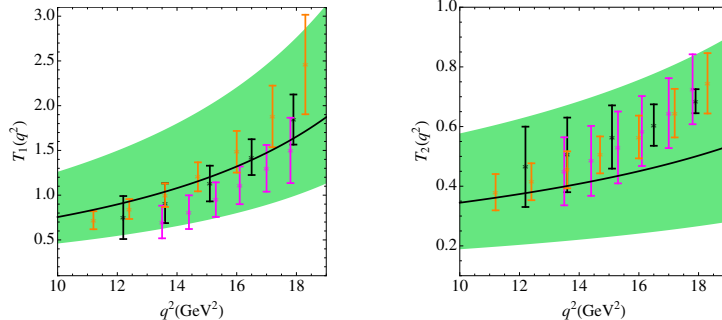
Low-recoil: LCSR are valid up to $q \leq 14 \text{ GeV}^2$. We extend FF determination [Bobeth & Hiller & Dyk'10] till 19 GeV^2 and cross check the consistency with **lattice** QCD.

In HQET one expects the ratios to be near one

$$R_1 = \frac{T_1(q^2)}{V(q^2)}, \quad R_2 = \frac{T_2(q^2)}{A_1(q^2)}, \quad R_3 = \frac{q^2}{m_B^2} \frac{T_3(q^2)}{A_2(q^2)}.$$

- BZ was problematic with R_3 .

Our approach: we determine $T_{1,2}$ by exploiting the ratios $R_{1,2}$ allowing for up to a 20% breaking, i.e., $R_{1,2} = 1 + \delta_{1,2}$. All other form factors extrapolated from KMPW.



- We find excellent agreement between our determination of $T_{1,2}$ using $R_{1,2}$ and lattice data.

Contact between theory and experiment:

Indeed the observables are measured in bins.

Present bins: [0.1,2], [2,4.3], [4.3,8.68], [1,6], [14.18,16], [16,19] GeV².

Comments on the bins:

- Ultralow bin region **[0.1,1]** including light-resonances analyzed in [S. Jager, JM Camalich]'12. Binning tends to wash out the resonances.
- The region $q^2 \sim 6 - 8.68$ GeV² can be affected by charm-loop effects. [Khodjamirian, Mannel, Pivovarov, Wang'10]
- The middle bin **[10.09, 12.89]** GeV² between J/ψ and $\psi(2s)$. Charm-loop effects lead to a destructive interference (raw estimate).
We treat it as a simple interpolation.
- Suggestion to experimentalists on binning: **[1,2], [2,4.3], [4.3,6]**

[S. Descotes, T. Hurth, JM, J. Virto'13], [J.M'12]

- Another possible source of uncertainty is the **S-wave contribution** coming from $B \rightarrow K_0^* l^+ l^-$ decay.
[Becirevic, Tayduganov '13], [Blake et al.'13]
- We will assume that both P and S waves are described by q^2 -dependent FF times a Breit-Wigner function.
- The **distinct** angular dependence of the S-wave terms in **folded** distributions allow to disentangle the signal of the P-wave from the S-wave: $P_i^{(\prime)}$ can be **disentangled** from S-wave pollution [JM'12].

Problem: Changing the normalization used for the distribution from

$$\frac{d\Gamma_K^*}{dq^2} \equiv \Gamma'_{K^*} \rightarrow \Gamma'_{full}$$

introduces a $(1 - \mathbf{F}_S)$ in front of the P-wave.

$$\Gamma'_{full} = \Gamma'_{K^*} + \Gamma'_S$$

and the longitudinal polarization fraction associated to Γ'_S is

$$\mathbf{F}_S = \frac{\Gamma'_S}{\Gamma'_{full}} \quad \text{and} \quad 1 - \mathbf{F}_S = \frac{\Gamma'_{K^*}}{\Gamma'_{full}}$$

The modified distribution including the **S-wave** and new normalization Γ'_{full} :

$$\begin{aligned}
\frac{1}{\Gamma'_{full}} \frac{d^4 \Gamma}{dq^2 d\cos\theta_K d\cos\theta_l d\phi} = & \frac{9}{32\pi} \left[\frac{3}{4} \mathbf{F_T} \sin^2 \theta_K + \mathbf{F_L} \cos^2 \theta_K \right. \\
& + \left(\frac{1}{4} \mathbf{F_T} \sin^2 \theta_K - \mathbf{F_L} \cos^2 \theta_K \right) \cos 2\theta_l + \frac{1}{2} \mathbf{P_1} \mathbf{F_T} \sin^2 \theta_K \sin^2 \theta_l \cos 2\phi \\
& + \sqrt{\mathbf{F_T} \mathbf{F_L}} \left(\frac{1}{2} \mathbf{P'_4} \sin 2\theta_K \sin 2\theta_l \cos \phi + \mathbf{P'_5} \sin 2\theta_K \sin \theta_l \cos \phi \right) \\
& - \sqrt{\mathbf{F_T} \mathbf{F_L}} \left(\mathbf{P'_6} \sin 2\theta_K \sin \theta_l \sin \phi - \frac{1}{2} \mathbf{Q'} \sin 2\theta_K \sin 2\theta_l \sin \phi \right) \\
& \left. + 2\mathbf{P_2} \mathbf{F_T} \sin^2 \theta_K \cos \theta_l - \mathbf{P_3} \mathbf{F_T} \sin^2 \theta_K \sin^2 \theta_l \sin 2\phi \right] (1 - \mathbf{F_S}) + \frac{1}{\Gamma'_{full}} \mathbf{W_S}
\end{aligned}$$

in the massless case and where the polluting terms are

$$\begin{aligned}
\frac{\mathbf{W_S}}{\Gamma'_{full}} = & \frac{3}{16\pi} \left[\mathbf{F_S} \sin^2 \theta_\ell + \mathbf{A_S} \sin^2 \theta_\ell \cos \theta_K + \mathbf{A_S^4} \sin \theta_K \sin 2\theta_\ell \cos \phi \right. \\
& \left. + \mathbf{A_S^5} \sin \theta_K \sin \theta_\ell \cos \phi + \mathbf{A_S^7} \sin \theta_K \sin \theta_\ell \sin \phi + \mathbf{A_S^8} \sin \theta_K \sin 2\theta_\ell \sin \phi \right]
\end{aligned}$$

We can get **bounds** on the size of the S-wave polluting terms.
Let's take for instance A_5

$$\mathbf{A}_S = 2\sqrt{3} \frac{1}{\Gamma'_{full}} \int \text{Re} \left[(A_0^{\prime L} A_0^{L*} + A_0^{\prime R} A_0^{R*}) BW_{K_0^*}(m_{K\pi}^2) BW_{K^*}^\dagger(m_{K\pi}^2) \right] dm_{K\pi}^2$$

where

$$\mathbf{F}_S = \frac{8}{3} \frac{\tilde{J}_{1a}^c}{\Gamma'_{full}} = \frac{|A_0^{\prime L}|^2 + |A_0^{\prime R}|^2}{\Gamma'_{full}} \mathbf{Y} \quad \mathbf{Y} = \int dm_{K\pi}^2 |BW_{K_0^*}(m_{K\pi}^2)|^2$$

\mathbf{Y} factor included to take into account the width of scalar resonance K_0^*

A bound is obtained once we define the $S - P$ interference integral

$$\mathbf{Z} = \int \left| BW_{K_0^*}(m_{K\pi}^2) BW_{K^*}^\dagger(m_{K\pi}^2) \right| dm_{K\pi}^2$$

and use the bound from the Cauchy-Schwartz inequality

$$\begin{aligned} & \left| \int (\text{Re}, \text{Im}) \left[(A_0^{\prime L} A_j^{L*} \pm A_0^{\prime R} A_j^{R*}) BW_{K_0^*}(m_{K\pi}^2) BW_{K^*}^\dagger(m_{K\pi}^2) \right] dm_{K\pi}^2 \right| \\ & \leq \mathbf{Z} \times \sqrt{[|A_0^{\prime L}|^2 + |A_0^{\prime R}|^2][|A_j^L|^2 + |A_j^R|^2]} \end{aligned}$$

From the definitions of F_S and F_L and P_1 one gets the following bound:

$$|A_S| \leq 2\sqrt{3}\sqrt{F_S(1-F_S)F_L} \frac{Z}{\sqrt{XY}}$$

the factor $(1 - F_S)$ in the bound arises due to the fact that F_L is defined with respect to Γ'_{K^*} rather than Γ'_{full} .

$$|A_S^4| \leq \sqrt{\frac{3}{2}}\sqrt{F_S(1-F_S)(1-F_L)\left(\frac{1-P_1}{2}\right)} \frac{Z}{\sqrt{XY}}$$

$$|A_S^5| \leq 2\sqrt{\frac{3}{2}}\sqrt{F_S(1-F_S)(1-F_L)\left(\frac{1+P_1}{2}\right)} \frac{Z}{\sqrt{XY}}$$

$$|A_S^7| \leq 2\sqrt{\frac{3}{2}}\sqrt{F_S(1-F_S)(1-F_L)\left(\frac{1-P_1}{2}\right)} \frac{Z}{\sqrt{XY}}$$

$$|A_S^8| \leq \sqrt{\frac{3}{2}}\sqrt{F_S(1-F_S)(1-F_L)\left(\frac{1+P_1}{2}\right)} \frac{Z}{\sqrt{XY}}$$

Coefficient	Large recoil ∞ Range	Low recoil ∞ Range	Large Recoil Finite Range	Low Recoil Finite Range
$ A_S $	0.33	0.25	0.67	0.49
$ A_S^4 $	0.05	0.10	0.11	0.19
$ A_S^5 $	0.11	0.11	0.22	0.23
$ A_S^7 $	0.11	0.19	0.22	0.38
$ A_S^8 $	0.05	0.06	0.11	0.11

Table : Illustrative values of the size of the bounds for the choices of F_S, F_L, P_1 and $\mathbf{F} = \mathbf{Z}/\sqrt{XY}$

- **Large-recoil:** $F_S \sim 7\%$ (like $B^0 \rightarrow J/\psi K^+ \pi^-$), $F_L \sim 0.7$ and $P_1 \sim 0$
- **Low-recoil:** $F_S \sim 7\%$, $F_L \sim 0.38$ and $P_1 \sim -0.48$.

We take the maximal value for Z/\sqrt{XY} factor in two cases:

“infinite range” \rightarrow integrals in the whole $m_{K\pi}$ range

“finite range” \rightarrow integrals around $m_{K^*} \pm 0.1$ GeV.

This may help in estimating the **systematics** associated to S-wave.

There is a correspondence between $\mathbf{P}_i^{(\prime)}$ and \mathbf{J}_k (β_ℓ^2 absorbed here in $F_{L,T}$)

$$\begin{aligned}
 (J_{2s} + \bar{J}_{2s}) &= \frac{1}{4} \mathbf{F}_T \frac{d\Gamma + d\bar{\Gamma}}{dq^2} & (J_{2c} + \bar{J}_{2c}) &= -\mathbf{F}_L \frac{d\Gamma + d\bar{\Gamma}}{dq^2} \\
 J_3 + \bar{J}_3 &= \frac{1}{2} \mathbf{P}_1 \mathbf{F}_T \frac{d\Gamma + d\bar{\Gamma}}{dq^2} & J_3 - \bar{J}_3 &= \frac{1}{2} \mathbf{P}_1^{\text{CP}} \mathbf{F}_T \frac{d\Gamma + d\bar{\Gamma}}{dq^2} \\
 J_{6s} + \bar{J}_{6s} &= 2 \mathbf{P}_2 \mathbf{F}_T \frac{d\Gamma + d\bar{\Gamma}}{dq^2} & J_{6s} - \bar{J}_{6s} &= 2 \mathbf{P}_2^{\text{CP}} \mathbf{F}_T \frac{d\Gamma + d\bar{\Gamma}}{dq^2} \\
 J_9 + \bar{J}_9 &= -\mathbf{P}_3 \mathbf{F}_T \frac{d\Gamma + d\bar{\Gamma}}{dq^2} & J_9 - \bar{J}_9 &= -\mathbf{P}_3^{\text{CP}} \mathbf{F}_T \frac{d\Gamma + d\bar{\Gamma}}{dq^2} \\
 J_4 + \bar{J}_4 &= \frac{1}{2} \mathbf{P}'_4 \sqrt{F_T F_L} \frac{d\Gamma + d\bar{\Gamma}}{dq^2} & J_4 - \bar{J}_4 &= \frac{1}{2} \mathbf{P}'_4{}^{\text{CP}} \sqrt{F_T F_L} \frac{d\Gamma + d\bar{\Gamma}}{dq^2} \\
 J_5 + \bar{J}_5 &= \mathbf{P}'_5 \sqrt{F_T F_L} \frac{d\Gamma + d\bar{\Gamma}}{dq^2} & J_5 - \bar{J}_5 &= \mathbf{P}'_5{}^{\text{CP}} \sqrt{F_T F_L} \frac{d\Gamma + d\bar{\Gamma}}{dq^2} \\
 J_7 + \bar{J}_7 &= -\mathbf{P}'_6 \sqrt{F_T F_L} \frac{d\Gamma + d\bar{\Gamma}}{dq^2} & J_7 - \bar{J}_7 &= -\mathbf{P}'_6{}^{\text{CP}} \sqrt{F_T F_L} \frac{d\Gamma + d\bar{\Gamma}}{dq^2}
 \end{aligned}$$

where each $\mathbf{P}_i^{(\prime)}$ and $\mathbf{P}_i^{(\prime)\text{CP}}$ encodes the information that can be extracted *cleanly* at large-recoil inside each \mathbf{J}_k and define the simplest possible fit besides S_i, A_i . The **brown** and **blue** pieces are strongly FF-dependent pieces.